ISSN: 2321-2152

IJMECE

International Journal of modern electronics and communication engineering

E-Mail
editor.ijmece@gmail.com
editor@ijmece.com

www.ijmece.com

ISSN2321-2152www.ijmece .com

Vol 11, Issue.4 Dec 2023

A Control Startegy for DC Grids Operations.

Mr.M.Srinivasulu [1],N.Sivakavitha [2], V.Pravalika[3],

Abstract—

In order to lessen the disturbance from PV production and the load fluctuation to the main grid without the need for a grid interface converter, a grid interface current control technique for a DC microgrid is proposed in this work. Within the DC microgrid, a battery DC-DC converter directly regulates the grid interface current. The control system has been theoretically modeled based on an extensive investigation of the battery DC-DC converter and interface current regulation. As a result, two transfer functions representing the inductor current's dynamic reaction to duty cycle variation (inner loop) and the grid interface current's dynamic response to inductor current variation (outer loop) could be generated. An experimental investigation was conducted to evaluate the efficacy of the suggested control approach. The experimental findings show that, despite differences in PV and load circumstances, the suggested control technique performs well in managing the grid interface current without the need for an interface converter.
Index Terms— Battery, DC microgrid, DC-DC converter, photovoltaic (PV) system.

I. INTRODUCTION

Modern power systems, which include energy storage devices, renewable energy sources, and novel load types like electric cars, depend heavily on distributed generation (DG). But in the absence of well-coordinated operation, it will lead to a number of problems for power systems, including reduced frequency reserves, transmission line congestion, and worsened voltage profiles [1]. Structured microgrids have been identified as the essential energy infrastructure for next smart energy systems in order to support greater distributed generation (DG) in power grids and lower carbon emissions. Direct current (DC) or alternating current (AC) lines may be used to connect microgrid components. In recent years, there has been a growing interest in DC energy systems research due to advancements in power electronics technology. Energy storage, DC electronics loads, and DC renewable production all naturally interact with DC-based energy systems [3]. DC systems provide greater economy, more dependability, and easier control than traditional AC systems [4-6]. The impact of a microgrid's renewable source on the functioning of the LV distribution network was examined in [7]. Utility voltage and line loss changes were analyzed by daily PV and load profile simulations. This study has provided important new information on how PV microgrids function in underpowered LV networks. The results showed that load variations and PV had an effect on the utility voltage. Line losses in the LV network were also noted. The authors concluded that in order to get rid of these variations, a sophisticated controller was necessary [7]. An interleaved interface converter was created in the research [8] in order to regulate the power flow between a DC microgrid and the DC bus of a main DC grid. Rather than just following the given reference, the controller was developed to be more successful in preventing PV and load disruptions. The PV and load fluctuations that are created inside a DC microgrid must be effectively handled in order to guarantee that the DC bus voltage stays at a consistent level.

Assistant Professor [1],
Department of EEE,

Sensitive loads may experience a series of voltage fluctuations as a result of these variations. However, in order to serve as the interface between the DC microgrid and the main DC grid for this research, a DC/DC interleaved converter is needed, which might raise the system's cost. A new method for power balancing that might be used to low voltage DC microgrids was introduced by the researchers in [9]. The goal of the research was to minimize the impact of PV output power oscillations on the main AC grid while still obtaining the MPP from the PV. Furthermore, a supervisory layer was created to maximize the battery energy storage system's (BESS) use and offset any voltage fluctuations brought on by the droop controller. Additionally, microgrids stand to gain a great deal from supply and demand involvement in pricing. As mentioned in [10], an aggregator is a company that gathers and sells the electricity produced by many microgrids.
electricity to the grid in an effort to drive down costs. Because of this, it is ideal for microgrids to provide electricity to the utility upon request from the aggregator, irrespective of fluctuations in load demand and the intermittent nature of renewable output. To make sure that PV and load disturbances are not transmitted to the main DC grid, a DC microgrid interface current control method is suggested in this research for the DC distribution network. There is no need for an extra interface converter between the DC microgrid and the main DC grid since the suggested interface current control method is based on the power converter control for the battery energy storage inside the DC microgrid. As a result, the system's expenses may be decreased without sacrificing the control performance shown in [8]. The remainder of this essay is structured as follows: The DC microgrid system configuration employed in this research is shown in Section II. Section III describes the system's tiny signal modeling. The compensator design and the suggested control technique are explained in Section IV. The experimental results are presented in Section V, and Section VI provides conclusions to wrap up the research.

II. CONFIGURATION OF THE DC MICROGRID SYSTEM

Fig. 1 displays the block diagram of the DC microgrid system used in this investigation. Without a grid interface converter, the DC microgrid is linked to the DC main grid. Since every converter in the DC microgrid operates in current mode, the whole DC microgrid is linked to the DC main grid in this mode. Power flow between the DC microgrid and the DC main grid may be regulated by adjusting the interface current Im. The PV array in the DC microgrid is linked to the DC bus by means of a Boost converter. Because the MPPT algorithm tracks the PV array's maximum power, the output power of the PV is dependent on the weather. The bi-directional DC-DC converter is used to connect the batteries to the DC bus. Direct connection of the load to the DC bus allows for user-controlled power usage. It is anticipated that as DC microgrid technology advance, many DC microgrids will link together to establish a DC main grid. A bi-directional DC/DC converter may be used to regulate the power flow between a DC microgrid and the main DC grid, as suggested in [8]. Alternatively, individual DC microgrids can be linked to the DC main grids in a variety of ways. A power inductor serves as the interface between the DC microgrid and the DC main grid in this research, as seen in Fig. 1. In order to regulate the grid interface current Im without the need for an interface converter, a control technique is put forward. For the purpose of controlling the grid interface current, fluctuations in PV current IPV and load current Iload are regarded as disturbances.

III. SMALL SIGNAL MODELLING AND ANALYSIS

Examining the bi-directional DC-DC converter's dynamic behavior is essential for batteries. This calls for the formulation and analysis of a small signal model of a bi-directional converter in addition to the regulation of the grid interface current between the main DC grid and the DC microgrid. This will make it possible to calculate two transfer functions that describe the dynamic responses of the grid interface current to the inductor current variation and the dynamic response of the battery convertor's inductor current to the duty cycle variation. The double loop PI compensators for the proposed control method will then be designed using two transfer functions. The charging and discharging modes of the bi-directional convertor use the same transfer function, as shown in [11]. Therefore, in scenarios when a single controller complements the two switches, a unified controller may be accepted. For the controller design in this research, the Boost operation mode has been used. Fig. 2 depicts the bi-directional DC-DC converter.

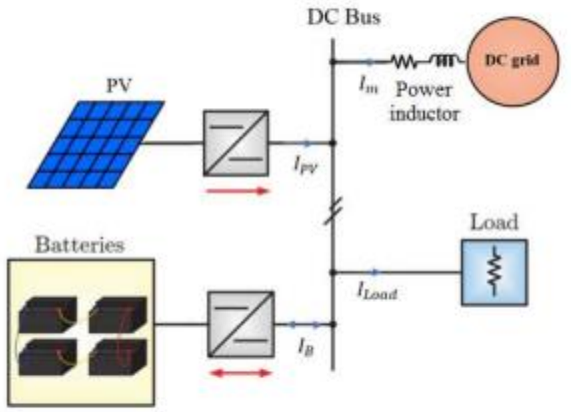

Fig. 1. The DC microgrid configuration for this study.

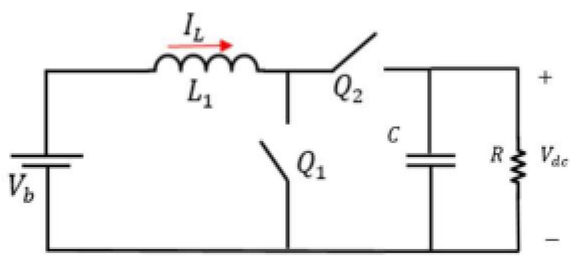

Fig. 2. The bi-directional DC-DC converter circuit diagram

The general average equation for the inductor voltage of the power converter can be derived as:

$$\frac{d\tilde{i}_L}{dt} = \frac{\tilde{v}_b + V_{dc}\tilde{d} - (1-D)\tilde{v}_{dc}}{L_1} \qquad (1)$$

$$\frac{d\tilde{v}_{dc}}{dt} = \frac{(1-D)\tilde{i}_L - I_L\tilde{d}}{C} - \frac{\tilde{v}_{dc}}{RC} \qquad (2)$$

where IL, C, R, and D represent the steady state variables of inductor current, capacitance and the load resistance of power converter, and duty cycle whereas, ± dc v , ° Li and d % denote the small signal perturbation variables of DC bus voltage, inductor current and duty cycle, respectively. To simplify the analysis, the battery voltage Vb can be assumed as a constant, so that v° b v is zero and can be ignored in the following analysis. The Laplace transfer function of Equations (1) and (2) can be represented as follows:

$$s\tilde{i}_L(s) = -\frac{1-D}{L_1}\tilde{v}_{dc}(s) + \frac{V_{dc}}{L_1}\tilde{d}(s) \qquad (3)$$

$$s\tilde{v}_{dc}(s) = \frac{1-D}{C}\tilde{i}_L(s) - \frac{1}{RC}\tilde{v}_{dc}(s) - \frac{I_L}{C}\tilde{d}(s) \qquad (4)$$

By rearranging equations (3) and (4), the transfer functions L) (/) (of the inductor current to duty cycle variation ° i s d s % and dc v s d s % can be) (/) (the DC bus voltage to duty cycle variation ± obtained:

$$\frac{\tilde{i}_L(s)}{\tilde{d}(s)} = \frac{V_{dc}Cs + 2I_L(1-D)}{L_1Cs^2 + \frac{L_1}{R}s + (1-D)^2} \quad (5)$$

$$\frac{\tilde{v}_{dc}(s)}{\tilde{d}(s)} = \frac{-L_1I_Ls + (1-D)V_{dc}}{L_1Cs^2 + \frac{L_1}{R}s + (1-D)^2} \quad (6)$$

Fig.3 shows a simplified diagram between the battery converter and the main DC grid. In this figure, Vdc depicts the DC bus voltage, IL represents the inductor current, Im denotes the grid interface current between the microgrid and the main DC grid, and Vm is the main DC grid voltage level. IR is the sum of the generation and load currents within the microgrid. When IR >0, it means the generation current is less than the load current, and when IR.

IV. THE PROPOSED CONTROL STRATEGY

The suggested interface current control technique regulates the grid interface current between the DC microgrid and the main DC grid by controlling the charge/discharge current of the battery to stop PV and load fluctuations from being transmitted to the main grid. For batteries, it is crucial to analyze the dynamic behavior of the bi-directional DC-DC converter. This necessitates controlling the grid interface current between the main DC grid and the DC microgrid in addition to developing and analyzing a tiny signal model of a bi-directional converter. This will enable the computation of two transfer functions that characterize the variations in the inductor current of the battery convertor and the grid interface current in response to changes in the duty cycle. Next, utilizing two transfer functions, the double loop PI compensators for the suggested control strategy will be created. The bi-directional convertor's charging and discharging modes, as shown in [11], use the identical transfer function. Consequently, a unified controller may be approved in situations when one controller enhances the other two switches. The Boost operation mode has been used to the controller design in this study. The bi-directional DC-DC converter is shown in Fig. 2.

To control the grid interface current Im a double loop interface current controller is developed, as shown in Fig.4. mref I is the reference current, which could be based on the request from an aggregator or a central controller. The reference current varies based on the request, but for a short period of time, it can be assumed as a constant. The proposed controller structure is similar to the double loop voltage control for a single Boost converter. The inner control loop is responsible for regulating the battery converter inductor current. Instead of controlling the output voltage, the outer control loop in this controller is responsible for regulating the grid interface current. The PV continually operates at maximum power point, and is therefore considered as a variable current source, whereas the DC load is regarded as a variable current sink.

The variables Gid, Gii, 1 Gpi , 2 Gpi , H1, and H2 represent the transfer function of the inner control loop, outer control loop, inner PI compensator, outer PI compensator, inner sensor and outer sensor, respectively. A comparison is made between the grid interface current Im and the reference current value mref I ; subsequently, the current error is delivered to the PI compensator 2 Gpi , which generates the required current Lref I for the inner control loop. A comparison is then made between the reference value Lref I and the inductor current IL and the current error is delivered to the PI compensator 1 Gpi . After this, the PI compensator generates the required duty cycle D, which is transferred to the PWM generator in order to create switching pulses that correspond to the battery converter. The bandwidth of the inner current controller is fixed at approximately fsw/10, where fsw represents the switching device switching frequency, which is 25 kHz for this study. The inner compensated control loop crossover frequency must be significantly lower than the main switching frequency. This is because the switching frequency can be rejected along with its related harmonics within the system control loop. Additionally, the outer control loop should have a slower response time in comparison to the inner control loop, as the former generates the reference for the latter and it must have greater speed to allow the inner control loop to track the generated reference by

ISSN2321-2152www.ijmece .com

Vol 11, Issue.4 Dec 2023

the outer control loop. Therefore, the bandwidth of the outer current control loop is maintained a level below that of the inner current control loop.

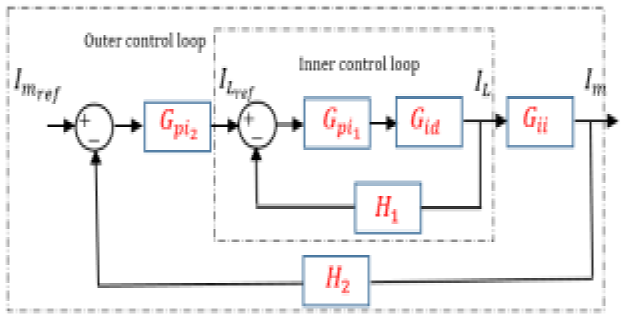

Fig.4. The proposed interface current control scheme.

EXPERIMENTAL RESULTS

The experimental setup shown in Fig. 9 was used to validate the performance of the proposed grid interface current control strategy. Fig.10 shows the block diagram of the experimental system setup. A battery pack, which has a voltage of 24 V, is connected to the DC bus using a bi-directional battery converter. The proposed grid interface current control was implemented in a TMS320F28335 microcontroller of the battery converter. A DC power supply at current source mode was used in this experiment to represent a PV generation. A DC electronics load was used to represent the DC load within the DC microgrid. Together with a branch resistor load, a DC power supply which has a voltage of 48 V was utilised to represent the main DC grid.
All data in the experiment were recorded using an oscilloscope (Wave Runner 104Xi-A). All specifications of the DC microgrid system are presented in Table II. To experimentally test the proposed grid interface control strategy performance, two cases are studied. A. Case1: Step Change in Load Current The objective of this case study is to assess the effects of load disturbances on the grid interface current control. The reference grid interface current value was set as 1A. As illustrated in Fig.11, the load current at t = t1 was suddenly raised from 0 A to approximately 0.5 A. Consequently, the Im (grid interface current) proportionally dropped from 1 A to around 0.5 A. In order to maintain the grid interface current Im at 1 A, the proposed controller increased the battery discharging current from 1 A to 1.5 A. At t = t2 the load current was returned to its original condition. To maintain the grid interface current at 1 A, the controller reduced the battery discharge current from approximately 1.5 A to 1 A. Fig.12 shows the zoom in the experimental waveforms that occurred at t = t1. This reveals that the grid interface current

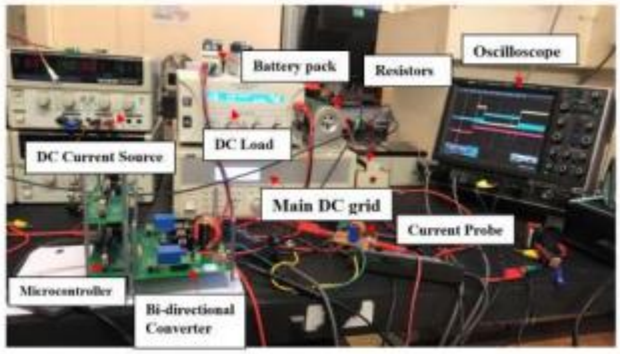

Fig.9. Experimental setup of the DC microgrid system.

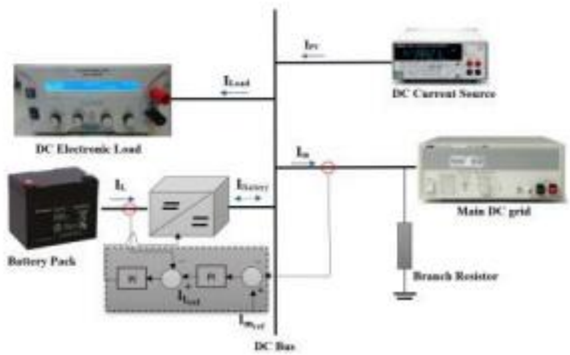

Fig.10.Schematic diagram of the complete DC microgrid system used in the experimental work.

TABLE II SPECIFICATION OF THE DC MICROGRID SYSTEM

Component	Type	Specification
DC power supply	GW Instek GPS-2303	2 A
Battery pack	YPC33-12×12	24 V
Main DC grid	QPX 1200S 1200-watt DC power supply	48 V
DC electronic load	EA-EL 2400-25	100 Ω
Branch resistors converter	-	10 Ω
Bi-directional converter	-	200W

Experienced a step change and then was regulated to 1 A after approximately 75 ms. The zoom in experimental waveforms at t = t2 is shown in Fig. 13. It shows that the grid interface current has a step change and then was regulated to 1 A after approximately 75 ms. The performance of the proposed control strategy was compared to that demonstrated in [8] which has an interface converter. It shows that the control in [8] has a different response time vary from 20 ms to 150 ms, which means that the proposed control strategy in this paper has similar performance as [8], and exhibits adequate performance in terms of the rejection of the load current disturbances, while effective regulation of the grid interface current can be achieved without an interface converter. B. Case2: Step Change in PV Generation The aim of this case study is to assess the effects of PV disturbances on the grid interface current controller. In the experiment, a reversed channel scope was used to read the PV current as the assumption was made that the direction of the PV current was opposite to that of the load current. As the PV current injects power to the DC bus, whereas, the load

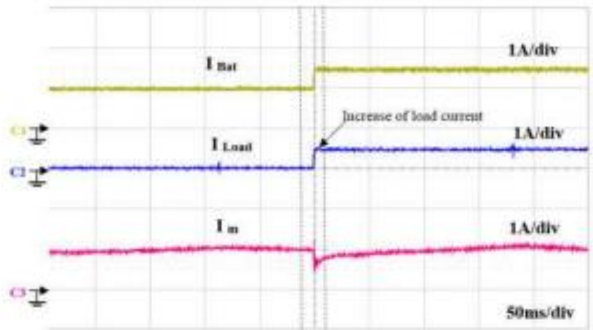

Fig.12. Experimental results for step change in load current under Zoom 1.

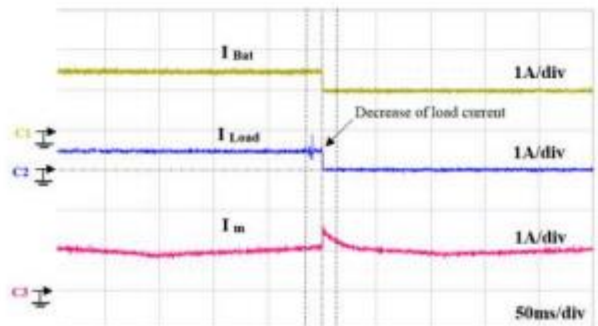

current consumes power from the DC bus. As shown in Fig.14, at the beginning, the PV current was 0 A, and the battery pack was discharged to supply the grid interface current of 1 A. At t = t1, the PV current was raised to 2 A. Consequently, the Im (grid interface current) is increased from 1 A to approximately 3 A. To maintain the grid interface current Im at 1 A, the battery was changed to operate in charging mode using a charge current of approximately 1 A for the purpose of absorbing the excess PV supply and regulating the Im according to its reference value. At t = t2, the PV current was returned to 0 A, and the battery worked as discharging mode with a discharge current of approximately 1 A. Fig.15 shows the zoom in experimental waveforms at approximately t = t1. It indicates that the grid interface current experiences a step increase change and is then regulated to 1 A after approximately 50 ms. Fig.16 illustrates the zoom in experimental waveforms at approximately t = t2. It indicates that the grid interface current experiences a step decrease change and is regulated after approximately 50 ms. The experimental findings indicate that the grid interface current Im was maintained at a constant level when variations in the PV current occurred. Hence, the proposed control strategy successfully prevented the PV variations from being transferred to the main DC grid.

V. CONCLUSIONS

Variations in renewable energy output and loads that are unpredictable might have a detrimental effect on the main grid. In this study, a DC microgrid grid interface current controller—which does not need a grid interface converter—was created to lessen the adverse impacts of PV production and load demand disruptions. A double loop grid interface current control is suggested after a thorough examination of the DC-DC converter and interface current control. The system transfer functions were used in the design of the inner and outer current compensators. The experimental findings support the suggested control strategy's efficacy.

REFERENCES

[1]. [1] A. Ipakchi and F. Albuyeh, "Grid of the future," in IEEE Power and Energy Magazine, vol. 7, no. 2, pp. 52-62, March-April 2009.

[2]. [2] D. Tan, "Structured microgrids: Ultimate assets for utilities," The 11th IET International Conference on Advances in Power System Control, Operation and Management (APSCOM 2018), 2018, pp. 1-7

[3]. [3] X. Yu, F. Wang and A. Q. Huang, "Power management strategy for plug and play DC microgrid," 2012 3rd IEEE PES Innovative Smart Grid Technologies Europe (ISGT Europe), Berlin, 2012, pp. 1-7.

[4]. [4] J. M. Guerrero, J. C. Vasquez, J. Matas, L. G. de Vicuna and M. Castilla, "Hierarchical Control of Droop-Controlled AC and DC Microgrids—A General Approach Toward Standardization," in IEEE Transactions on Industrial Electronics, vol. 58, no. 1, pp. 158-172, Jan. 2011.

[5]. [5] D. Salomonsson, L. Soder and A. Sannino, "Protection of Low-Voltage DC Microgrids," in IEEE Transactions on Power Delivery, vol. 24, no. 3, pp. 1045-1053, July 2009.

[6]. [6] R. M. Cuzner and G. Venkataramanan, "The Status of DC Micro-Grid Protection," 2008 IEEE Industry Applications Society Annual Meeting, Edmonton, AB, 2008, pp. 1-8.

[7]. [7] Zehir et al., "Impact of Renewable Based Microgrid Supply/Demand Profiles on Low Voltage Distribution Networks", Energy Procedia, vol. 103, pp. 231-236, 2016.

[8]. [8] Tricarico, T.; Gontijo, G.; Neves, M.; Soares, M.; Aredes, M.; Guerrero, J.M. Control Design, Stability Analysis and Experimental Validation of New Application of an Interleaved Converter Operating as a Power Interface in Hybrid Microgrids. Energies 2019, 12, 437.

[9]. [9] M. Mobarrez, S. Bhattacharya and D. Fregosi, "Implementation of distributed power balancing strategy with a layer of supervision in a low-voltage DC microgrid," 2017 IEEE Applied Power Electronics Conference and Exposition (APEC), Tampa, FL, 2017, pp. 1248-1254.

[10]. [10] H. Kim and M. Thottan, "A two-stage market model for microgrid power transactions via aggregators", Bell Labs Technical Journal, vol. 16, no. 3, pp. 101-107, 2011.

[11]. [11] S. K. Kollimalla, M. K. Mishra and N. L. Narasamma, "Design and Analysis of Novel Control Strategy for Battery and Supercapacitor Storage System," in IEEE Transactions on Sustainable Energy, vol. 5, no. 4, pp. 1137-1144, Oct. 2014.